[AMERICAN JOURNAL OF SCIENCE, VOL. 277, APRIL, 1977, P. 384-414]

NUMERICAL ANALYSIS OF LAVA LAKE COOLING MODELS: PART I, DESCRIPTION OF THE METHOD

HERBERT R. SHAW,* MARGARET S. HAMILTON,** and DALLAS L. PECK**

ABSTRACT. A computer method for numerical solution of problems in transient heat flow has been developed and applied to cooling models of Hawaiian lava lakes. This report and part II by Peck, Hamilton, and Shaw apply the method to Alae lava lake as the first detailed test against a systematic program of temperature measurements in lava lakes carried out by the Hawaii Volcano Observatory. The method is neither a finite element nor finite difference method, as the terminology of numerical analysis is currently employed, though there are similarities to both. It is an adaptation of a computer method that we call the method of explicit cell balances. Input-output balances are computed between cells in a grid system simulating the lava lake geometry. Computation explicitly performs the cell balances sequentially in the same way the "cooling wave" moves into the lava body without recourse to numerical solutions of sets of simultaneous equations. The procedure clearly identifies the physical processes governing thermal effects: the effects of the latent heat of crystallization, effects of rainfall permeating the lava surface, and effects of large variations in density and thermal conductivity. The accuracy of numerical approximations was tested against exact solutions for an extrusive sheet without sources. Deviations were less than 1°C in all cases. Agreement with data for Alae lava lake given in part II indicates that the method can be used with good confidence for refinement of thermal properties and identification of heat transfer mechanisms in other lava lakes as well as for predictive tests of cooling histories for hypothetical systems involving complicated heat transfer mechanisms.

INTRODUCTION

Thermal and petrogenetic studies of Kilauean lava lakes have been a consistent interest of the Hawaii Volcano Observatory, associated members of the U.S. Geological Survey, and many collaborators from all over the world since 1960, after the filling of Kilauea Iki crater during the 1959-1960 eruption of Kilauea volcano. Study of that large lava lake still continues, and the results of other studies of lava lakes are outlined in a review by Wright, Peck, and Shaw (1976).

The present report describes a method of numerical analysis of cooling histories and gives a comparison with previous results from exact solutions of the differential equations of heat flow. The method is illustrated by application to Alae lava lake, which formed during the 1963 eruption of Kilauea; a detailed discussion of the thermal history of Alae lake is given in part II by Peck, Hamilton, and Shaw and by Peck (in press). Alae is the thinnest and has the smallest volume of any of the lakes studied; hence it cooled the fastest and corresponded the most closely to cooling of an extrusive sheet. Temperatures were measured in drill holes in this lake for a 4-year period beginning September 1963, during which time the maximum temperature had fallen to less than 100°C.

The approach taken in this report is first to compare the results of simplified numerical analysis of cooling with the existing measured temperature profiles, then to reduce the difference between calculated and

* U.S. Geological Survey, Menlo Park, California 94025
** U.S. Geological Survey, National Center, Reston, Virginia 22092

observed temperature distributions by incorporating estimates of heat sources and sinks and variations of density, thermal conductivity, and heat capacity. Although we experimented briefly with two-dimensional analysis, we found that, because of the small ratio of thickness to lateral extent in both horizontal dimensions, a one-dimensional analysis was quite adequate to describe all but the subtlest details of cooling as represented by the observational data. Computations in two or three dimensions are conceptually no more difficult, though all aspects of computer runs become increasingly time-consuming and costly.

Questions have plagued past discussions of cooling of lava lakes. Among the first emphasized was the effect of rainfall on the surface (Richter and Moore, 1966). Subsequently, questions have arisen concerning the effects of variable conductivity and magmatic convection on the details of cooling histories. The principal incentive for our study was to find a method of analysis sufficiently flexible to test the possible magnitudes of the above secondary effects. From the standpoint of total cooling times, we find that vaporization of rainwater and variations of diffusivity produce the major differences from earlier results derived from applications of conduction theory using constant physical properties (Peck, Moore, and Kojima, 1964; Jaeger, 1968). We point out, however, that from the standpoint of petrogenetic evolution of large magma bodies, other effects of mass transfer such as convection, crystal settling, vesiculation, or filtration of pore liquids at late stages of crystallization are of great importance to quantitative ideas concerning the detailed history of heat transfer. The method of explicit cell balances described below offers a flexible approach to assessments of the relation between the total amount of magmatic heat and the heat distributed in complicated ways within the magma chamber and in surrounding rocks. The ability to describe the thermal effects of igneous processes will govern any future possibilities of extracting mechanically useful energy from magmatic systems and will provide the principal criterion of whether or not that extraction may produce serious imbalances in related geologic systems from an environmental standpoint.

We anticipate the results described in part II of this article by Peck, Hamilton, and Shaw to say that the temperature data for Alae can be reproduced within the precision of measurement by systematic allowance for latent heat of crystallization, vaporization of rain, and variations of thermal diffusivity. It was found that representative temperature profiles prior to complete solidification could be fitted to within an average deviation of 20°C without assuming any convective mixing of the melt. This implies that heat transfer was dominantly conductive, although small components of convective heat transfer could not be tested because the above agreement is near the resolution of temperature data. This conclusion, however, does not generally apply to other lava lakes or to magmatic intrusions. Data for thicker lava lakes are now being analyzed as further tests of heat transfer mechanisms.

PREVIOUS STUDIES

The principal approach to calculations of heat transfer in crustal rocks has employed the analytic methods of conduction theory closely following the methods of Ingersoll, Zobel, and Ingersoll (1954) and Carslaw and Jaeger (1959). Specific application to magma bodies mainly reflects studies such as those of Boydell (1932), Lovering (1955), Larsen (1945), Rikitake (1959), Reilly (1958), and Jaeger (1957, 1964, and 1968). Little consideration was given to questions of magma convection in these studies, perhaps because the maximum effect of complete mixing is not of major significance to total cooling times in order-of-magnitude calculations (Jaeger, 1968; Shaw, 1974). Some of the consequences of magmatic convection have been qualitatively discussed in many papers (for example, H. H. Hess, 1960; Shaw, 1965), and a few quantitative estimates of convective effects have been attempted (for example, McBirney, 1959; Shaw, 1965, 1974; Irvine, 1970; G. B. Hess, 1973). Convective mixing of the melt was assumed by Provost and Bottinga (1972) in a numerical analysis of rates of solidification of lunar basalt flows and Hawaiian lava lakes. This assumption combined with a radiation boundary condition at the upper surface and different thermal properties might suggest that their results would be considerably different from ours. The existing similarity (see Provost and Bottinga, 1972, fig. 5) indicates that the two different sets of assumptions involve compensating effects relative to deviations from cooling times for simple conduction models.

Numerical analysis of data for Alae lava lake was begun by Jaeger in 1966, but the results were not published. He used a combination of analytic and finite difference approximations with different sets of constant physical properties to compare with the temperature measurements supplied to him by one of us (Peck; Jaeger, written commun., 1967). The method of analysis differs importantly from that described here; later we will illustrate some of the differences in approach and results.

CHOICE OF ANALYTICAL METHOD

Nearly all studies of igneous cooling histories have relied on mathematical solutions of the differential equations of heat conduction. In some cases where solutions to the equations were not known, a finite difference formulation was used to augment the scope of the exact solutions (Jaeger, 1957; Carslaw and Jaeger, 1959). Other methods such as graphical and analog analysis have been used in engineering practice (McAdams, 1954; Hsu, 1963) but have not seen wide application in geology. The former method is slow and laborious, whereas the latter approach effectively requires construction of some physical model analogous to the system of interest.

The method of numerical analysis we have adopted has some important advantages over other methods. Geologically, the main advantage is that it describes what is happening physically within the model system without recourse to the formal and sometimes obscure operations of differential calculus. The only assumptions necessary are conservation of

mass and energy and the validity of Fourier's law of heat conduction, which states that heat flow is proportional to the gradient of temperature. Account is taken of complex processes without the necessity of introducing mathematical operations that make the solution of differential equations effectively impossible. Other advantages are that there is virtually no restriction on the shape of the system considered, nor are there any restrictions on the distribution of physical properties or the kinds and distributions of heat sources and sinks.

In the descriptive sense, the term finite element analysis would seem appropriate, because we are dealing with an array of finite elements or cells of prescribed geometries and thermal properties. The current practice of numerical analysts, however, appears to restrict the term "finite element analysis" to a specific extension of Rayleigh-Ritz-Galerkin techniques (Desai and Abel, 1972; Strang and Fix, 1973). Therefore, we will refer to our approach as the "method of explicit cell balances." It is a direct outgrowth of techniques described by Davids and Berger (1964) and Berger and Davids (1965).

A possible disadvantage of the method is that it computes changes in each element or cell in sequence rather than solving matrices of simultaneous equations as is done in other finite difference methods. This is valuable in the descriptive sense, because it is easy to follow the changes in the system, as it "relaxes" from a prescribed initial state toward some final set of boundary conditions. However, if the problem is too intricate in terms of number of cells, the computer time required for approach to the desired limit may be prohibitive. In such problems, an unconditionally stable finite difference scheme such as the alternating-direction-implicit method of Peaceman and Rachford (1955) might be better using a coarse grid as a reconnaissance tool to identify conditions that might be refined by the explicit method.

CELL BALANCE FORMULATION OF HEAT TRANSFER MODELS

Heat balance equations.—The steps involved in the computation are so straightforward that flow diagrams or sample programs are not necessary for duplication of the computer results. Information on the actual programs used can be obtained by contacting the authors. Our notation was chosen to be as explicit as possible on the meaning of terms and to be consistent with symbols available for printout of computer runs. To avoid confusion between text symbols and computer symbols, we decided to retain the latter throughout, specifically the use of U for temperature and T for time.

The simplicity of the method is based on the fact that heat conduction computations can be described in terms of the following two fundamental equations, stated for a one-dimensional model divided into a number of cells or elements of length ΔX_i and unit cross-sectional area:

$$\Delta Q_{i+1} = K_i(U_{i+1}-U_i)\frac{\Delta T}{\Delta X_i} \quad \text{(Fourier's Law)} \qquad (1)$$

$$\Delta U_i = \frac{(\Delta Q_{i+1} - \Delta Q_i)}{P_i C_i V_i} + \frac{\Delta Q_i^*}{P_i C_i V_i} \quad \text{(Thermal Energy Balance)} \qquad (2)$$

where K is conductivity, P is density, C is heat capacity, and V is cell volume. The term ΔQ_{i+1} is derived from Fourier's law and defines the increment of heat crossing the boundary between cells i and i+1 during a specified time increment ΔT; ΔU_i is the change of mean temperature of cell i required by conservation of energy within the cell for increments of heat gained from and lost to neighboring cells as well as any produced or absorbed within the cell (for example, by chemical reactions) during the same time increment, symbolized by ΔQ_i^*. For computations in two or three dimensions, eq (1) includes terms for heat transfer across the additional cell faces.

In our formulation, thermal properties of each cell are mean values, and *mean temperatures are plotted at cell centers;* numerical analysis, in general, permits properties to be specified at either central or nodal points. Strictly speaking from this standpoint, if conductivity K strongly varies with either temperature or position, the values should be averages for adjoining cells. Considerations of this nature emerge as analysis proceeds and are easily incorporated by adjustments of the program.

There is great flexibility in the method for incorporation of effects caused by processes other than simple phonon conductivity. For example, if evidence suggested that either radiative or convective heat transfer may have been important in the thermal history, eq (1) might be modified to give heat transfer coefficients in terms of "effective conductivities" as functions of temperature, temperature gradients, position, or other variables. These "effective conductivities" might incorporate other local properties that influence the heat transfer (thermal emissivity, density, or viscosity). Analogously, eq (2) might be modified to account for various forms of heat sources and sinks. These source-sink balances can be specified at boundaries, uniformly, arbitrarily in each cell, or as functions of physical changes in the system during a computer run.

Examples of source-sink balances generally pertinent to geological calculations are heat produced by radioactivity, heat produced by exothermic reactions (crystallization of a melt), heat consumed by endothermic reactions (vaporization of a liquid), or heat produced by some form of dissipation of mechanical energy. Application to simple cases of heat generation caused by flow of viscous liquids is demonstrated by Siekierka (1971), following the ideas of thermal feedback described by Gruntfest (1963) and Shaw (1969).

The terms ΔQ_i and ΔQ_{i+1} in eq (2) incorporate the net effects of the "effective conductivities" of eq (1), whereas the quantities ΔQ_i^* incorporate the net effects of all source-sink balances.

The computer equations in terms of thermal diffusivity.—Eqs (1) and (2) involve the three properties: thermal conductivity K_i, density P_i, and heat capacity C_i. Although the general magnitudes of these quan-

tities for lavas are known, each varies independently in each cell as functions of temperature and time. These variations can be as large as a factor of two or more for conductivity and density; heat capacities vary mainly according to temperature and the modal composition of a cell and can be predicted with good confidence from thermochemical data.

As one of the purposes of the numerical analysis was to derive a self-consistent set of properties for Alae lava, it was simplest first to attempt solutions only in terms of a constant thermal diffusivity, $D_i = K_i/P_iC_i$, thereby reducing the number of property variables to one. Given a set of thermal diffusivity values versus temperature, depth in the lake, and time, the resulting set of D_i values was then compared with the known distributions of densities and calculated heat capacities to test for the range of variations of apparent conductivities. We say "apparent conductivities" because the conductivity so derived includes any contributions from radiative or convective heat transfer. This aspect of the problem is discussed in part II of this article. The results, however, are shown to be internally consistent within the uncertainties of measurement of the above properties for basaltic lava.

Alternatively, if the aim is to test for temperatures predicted according to specific relations with K_i, P_i, and C_i, these can be introduced independently. An example might be to use values predicted by the Alae lake correlations as an input for analysis of a thicker lava lake to test for possible convective contributions of significant magnitudes.

The two operational equations in terms of thermal diffusivity are written

$$LUV_{i+1} = D_i(U_{i+1} - U_i)\frac{\Delta T}{\Delta X_i} \quad \text{(Fourier's Law)} \tag{3}$$

$$\Delta U_i = \frac{(LUV_{i+1} - LUV_i)}{V_i} + \frac{LUV_i^*}{V_i}, \quad \text{(Thermal Energy Balance)} \tag{4}$$

where LUV_i is simply a computer code for the quantity $\Delta Q_i/P_iC_i$. Near the upper cooling surface, the quantity LUV_{i+1}/V_{i+1} is the amount by which the temperature would be lowered in cell i+1, and LUV_{i+1}/V_i is the amount by which it would be raised in cell i, for flow of an increment of heat ΔQ_{i+1} from cell i+1 to cell i; the sign of the heat flow increments is reversed at positions below the maximum temperature in the lake.

The sign conventions are written so that heat flow to the upper surface is positive; a simplified model is shown in figure 1 and described in the next section. Cells are numbered consecutively downward from the upper surface of the lake, and, in general, the ΔU_i values are negative; that is, conventions are for a cooling model. The quantity LUV_i^*/V_i is the analogous effect on temperature of a heat source or sink in cell i. LUV^*_i is positive for the latent heat of crystallization and negative for

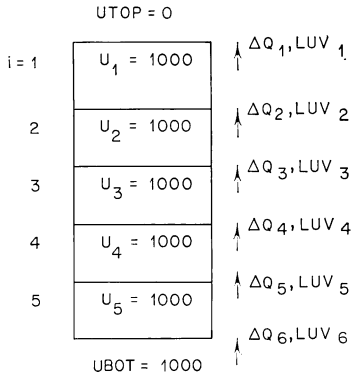

Fig. 1. Arbitrary example in one dimension illustrating the initial conditions of a calculation for a 5-cell model with unit values of D_i and ΔX_i and constant boundary temperatures. Heat flow measurements after the start of the calculation are indicated schematically on the right. The increments ΔQ_1 and ΔQ_6 imply the existence of an additional imaginary cell respectively above and below the top and bottom boundaries.

the heat of vaporization of rainwater. Note that for a one-dimensional model with equal cell lengths, $V_i = \Delta X_i$.

Even though we are dealing with a cooling model, the complex history of vaporization of rain could conceivably cause transient reversals in temperature gradients in the upper part of the lake so that ΔU_i could be transiently positive in some cells. Therefore, we did not constrain the ΔU_i to be negative as might be done as a stability test in a system that is required to cool monotonically in all cells. The effect of increments of the latent heat crystallization, of course, is to give positive increments to the ΔU_i in those cells above the solidus temperature. Because of the way LUV_i* is defined for crystallization, however, this heat source cannot cause a net increase of temperature in a cell and, therefore, does not itself introduce possibilities of numerical instability. Definition of the source-sink terms and tests for numerical stability are given in a later section.

Simplified example of a computer run for given initial and boundary conditions.—Because the method of cell balances is a form of relaxation analysis, it has often been applied only to changes from a specified initial state to a final equilibrium state or steady state. In heat transfer problems, this application is represented by relaxation from an initially specified temperature distribution to a final steady temperature distribution; one example is the approach to a final linear temperature gradient in a sheet of constant conductivity when the temperature of one or both surfaces is changed from the initial temperature and is held at some different constant temperature. The cooling of a lava flow is similar to this problem, except that heat flow from the bottom surface enters a semi-infinite medium, whereas the top surface is held at an effectively constant temperature. Although both cases are forms of transient heat flow, the latter *has no* fixed limiting condition at the bottom surface. For practical purposes, however, the lower boundary condition poses no problem, because

temperature changes within and below the sheet can be computed to any desired accuracy by specifying an arbitrarily constant ambient temperature at some relatively large distance below the bottom surface.

In order to focus the discussion, a simple calculation will be described for a sheet with no heat sources and constant contact temperatures. Figure 1 shows an arbitrary one-dimensional 5 cell grid to illustrate the initial conditions of the calculation and the meaning of terms described above. Initially, the sheet has a uniform temperature of 1000 degrees (any non-uniform distribution could have been specified), and, at time zero, the upper surface is changed to and held at zero degrees, while the bottom surface is held constant at 1000 degrees. In this example, the thermal properties and cell properties and cell lengths are given unit values, and the boundaries are held at constant temperature so that the initial steps of the calculation are easily identified. The first few cooling increments of this model would correspond to the initial cooling of the top surface of a lava lake. In the real situation, of course, the bottom boundary conditions are modified to allow also for cooling from below, as described later, and the initial temperatures are different.

In order to start the calculation, a time increment must be chosen. The increment should be large enough that the computation is efficient but not so large that unstable or meaningless solutions are obtained. For example, too large a value of ΔT in eq (1) could give a heat flow increment that would predict a temperature depression greater than 1000 degrees. In the absence of a negative heat source, this violates laws of thermal equilibrium and would produce unstable oscillations of heat flow with increments flowing in opposite directions.

The question of "computational stability" has been much discussed relative to methods of numerical analysis (for example, Price and Slack, 1954). A generally accepted test for stability is described by the so-called modulus condition (Carslaw and Jaeger, 1959; Davids and Berger, 1964):

$$M = D_i \frac{\Delta T}{\Delta X_i^2} \leqslant \frac{1}{4} . \tag{5}$$

For unit values of D_i and ΔX_i this gives $\Delta T \leqslant 0.25$, measured in the consistent time unit.

Obviously, for purposes of comparing calculated with observed thermal histories, it might be desired to specify ΔT rather than ΔX_i. If so, the modulus condition identifies the grid size consistent with that choice. In heterogeneous systems, it is possible that the modulus condition is satisfied in some cells and not in others. Instability can be avoided in such cases by specifying in the program that cells in which $M > 0.25$ have attained thermal equilibrium (see Davids and Berger, 1964).

The first cooling increments are computed from eqs (3) and (4) by introducing $\Delta T = 0.25$ in eq (3) for each cell in sequence and then intro-

ducing the resulting values of LUV_i in eq (4) in sequence to obtain ΔU_i, as follows:

Time Step One

$$LUV_1 = D(U_1 - UTOP)\frac{\Delta T}{\Delta X} = 1(1000 - 0)\frac{0.25}{1} = 250$$

$$LUV_2 = D(U_2 - U_1)\frac{\Delta T}{\Delta X} = 1(1000 - 1000)\frac{0.25}{1} = 0$$

$$LUV_3 = LUV_4 = LUV_5 = LUV_6 = 0$$

$$\Delta U_1 = \frac{LUV_2 - LUV_1}{V_1} = \frac{0 - 250}{1} = -250$$

$$\Delta U_2 = \frac{LUV_3 - LUV_2}{V_1} = 0$$

$$\Delta U_3 = \Delta U_4 = \Delta U_5 = 0$$

From these initial values of ΔU_i, the adjusted temperatures are assigned to each cell, and computations from eqs (3) and (4) are repeated:

Time Step Two

$$U_1 = 1000 - 250 = 750;\ U_2 = 1000, \text{ et cetera}$$

$$LUV_1 = D(U_1 - UTOP)\frac{\Delta T}{\Delta X} = 1(750 - 0)\frac{0.25}{1} = 187.5$$

$$LUV_2 = D(U_2 - U_1)\frac{\Delta T}{\Delta X} = 1(1000 - 750)\frac{0.25}{1} = 62.5$$

$$LUV_3 = LUV_4 = LUV_5 = LUV_6 = 0$$

$$\Delta U_1 = \frac{62.5 - 187.5}{1} = -125$$

$$\Delta U_2 = \frac{0 - 62.5}{1} = -62.5$$

$$\Delta U_3 = \Delta U_4 = \Delta U_5 = 0$$

The above steps continue to be repeated as long as desired. Sample calculations with and without heat sources can be done by hand for a few time steps to get a feel for the way temperature distributions begin to evolve. A positive heat source simply adds a temperature increment to changes of ΔU_i (that is, cooling is slowed by the latent heat of crystallization; actual heating is possible for large sources such as might be caused by dissipation of mechanical energy in non-static systems), and a negative source augments cooling. Table 1 gives a numerical display of the results of the above hand calculation, and figure 2 illustrates the calculated temperature profiles.

Two problems are indicated by figure 2 relative to the accuracy of incremental calculations. One is that the number of time steps required

to reach the steady state gradient is effectively infinite, because the rates of cooling eventually slow with time. This is not a serious practical problem with the availability of high-speed computers, but it does indicate that if the principal interest is in the final stages of cooling, an exceedingly fine grid is inefficient. If interest is in both early and late stages, the cell size can be made to increase with time. This condition could be written into the program so that the time steps calculated from eq (5) will increase, for instance, as the square of the chosen cell lengths.

A more serious problem indicated by figure 2 is the question of temperature ambiguity caused by the finite cell length, especially at a boundary where thermal properties change or where a constant temperature is imposed. For example, the calculation assumed the existence of an imaginary cell with the same thermal properties above the first cell, and because temperatures are plotted at cell centers, the profile does not converge to $U = 0$ at the top surface. Practically, this uncertainty is minimized by making cell sizes small enough that the plotting error is not significant. Alternatively, the profile can be forced to fit $U = 0$ at the surface with initial heat flow increments ΔQ_1 calculated on the basis of half the cell length in the first cell. In some cases, real heat transfer coefficients could be assigned to the cooling medium (for example, air, or water in the case of submarine lava flows) and temperature profiles calculated across the contact. In the analysis of the lava lake data, however,

TABLE 1

Numerical results of calculation for example in figure 1*

T	*UTOP*	*LUV*$_1$ U$_1$	*LUV*$_2$ U$_2$	*LUV*$_3$ U$_3$	*LUV*$_4$ U$_4$	*LUV*$_5$ U$_5$	*LUV*$_6$ U$_6$
0	0	1000	1000	1000	1000	1000	1000
		← 250	0	0	0	0	0
0.25	0	750	1000	1000	1000	1000	1000
		← 187.50	← 62.50	0	0	0	0
0.50	0	625	938	1000	1000	1000	1000
		← 156.30	← 78.10	← 15.60	0	0	0
0.75	0	547	875	984	1000	1000	1000
		← 136.70	← 82.05	← 27.35	← 3.90	0	0
1.00	0	492	820	961	996	1000	1000
		← 123.04	← 82.04	← 35.16	← 8.79	← 0.98	0
1.25	0	451	773	935	988	999	1000
		← 112.79	← 80.57	← 40.29	← 13.43	← 2.68	← 0.25
1.50	0	419	733	908	978	997	1000
		← et cetera	←	←	←	←	←
	0						

*For unit values of D_1 and ΔX_1 in the metric system, time is in seconds. The temperature scale is arbitrary. Values are tabulated for 6 time steps during which time the cooling wave has penetrated to the fifth cell. At time step 6, heat begins to flow into the sheet from the subjacent region held at a constant temperature of 1000 degrees. Temperatures are rounded to the nearest integer. Care must be taken during the computation, however, to carry enough significant figures to avoid an accumulation of rounding errors.

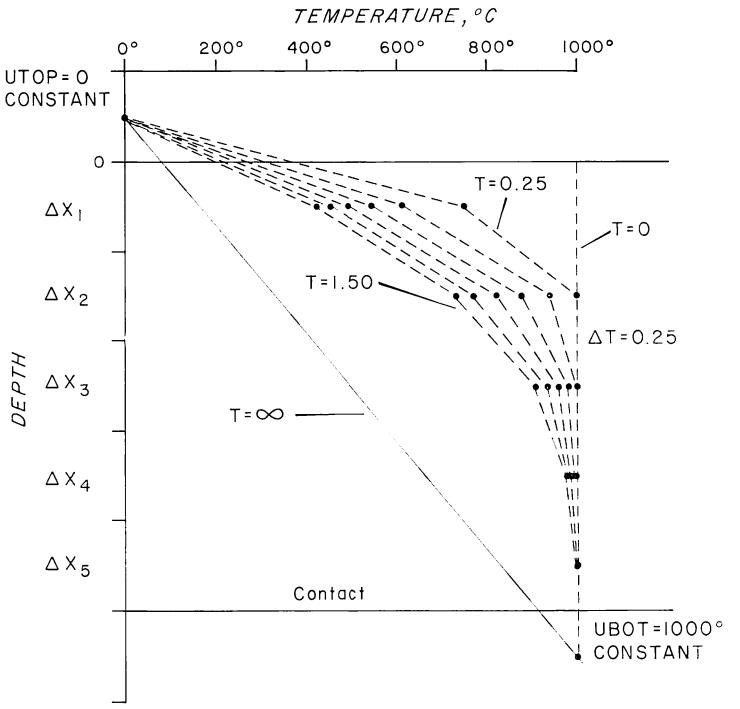

Fig. 2. Plot of computed temperatures from table 1 for arbitrary 5-cell model of infinite sheet with unit values of D_i and ΔX_i.

the half-cell length assumption was used for the first cell; temperatures at the bottom contact are determined by interpolation.

Comparison of numerical and exact solutions for the infinite sheet without heat sources.—In order to test the accuracy of our numerical calculations, a series of runs was made for the case of an extrusive sheet without sources, in various combinations of cell sizes and bottom boundary conditions. Exact solutions for the sheet with uniform properties are illustrated in many references (see Jaeger, 1968). For the sake of graphical comparisons, we chose the example illustrated by Ingersoll, Zobel, and Ingersoll (1954, p. 99, fig. 7.5). If very detailed numerical comparisons are desired, the exact solution can be simultaneously computed and displayed, either numerically or on the same computer plot with the numerical results.

The example is a sheet 20 m thick with a thermal diffusivity of 0.0118 cm^2sec^{-1}. To illustrate the magnitudes of errors, we assume an initial temperature of 1000°C and upper and lower contacts at 0°C. The maximum temperature computed analytically begins to fall below 1000°C in about 3 model months, reaches about 660°C in a yr, and falls to about 120°C in 9 model yrs. During this time, the position of the maximum temperature, which in the early stages of cooling is near the center of the

sheet, progressively increases in depth until it is approximately at the lower contact after 9 yrs. The reason, of course, is that heat loss from the upper contact, which is held at 0°C, far exceeds heat loss from the lower contact, which is initially at 0°C but rises to half the magma temperature immediately after emplacement. Because of this asymmetric cooling, the lower boundary condition is very important for finite element analysis, if temperatures are to be calculated near or below the bottom contact of the sheet.

As stated above, we imposed an artificial lower boundary condition by specifying a constant temperature at some distance below the bottom contact — we designate this temperature as *UINF*. Initially, we divided the sheet into 10 cells and placed the *UINF* plane at half the sheet thickness below the bottom contact (that is in cell i = 16). We used time steps calculated from the modulus condition M = 0.25 (eq 5) and plotted temperature profiles at 3 months and at intervals of 1 yr to 9 yrs (Ingersoll, Zobel, and Ingersoll, 1954, give profiles at 3 months, 1, 4, and 9 yrs).

With the 10 cell grid and *UINF* = 0 in cell 16, calculated temperatures in the upper part of the sheet were as much as 100°C too high at 3 months and about 50°C too high at 1 yr, whereas temperatures at the lower contact were nearly correct up to 1 yr but were about 100°C too low after 9 yrs. Placing *UINF* = 0 at two sheet thicknesses below the lower contact and maintaining the 10-cell grid within the sheet gives lower contact temperatures within about 10°C of the correct values throughout the 9 yr history. Temperatures in the upper part of the sheet, however, still have about the same errors.

Next, we maintained *UINF* at 0 at two sheet thicknesses below the contact and increased the number of cells within the sheet to 20 and then to 40. The 20-cell model reduced the errors in the upper part of the sheet to about 20°C above the analytic values, and in the 40-cell model temperatures calculated by the two methods are so nearly identical that the profiles are indistinguishable within the resolution of graphical display. Figure 3 shows the computer drawn result for the 40-cell model. Direct comparisons of numerical printouts showed that temperatures agreed to within less than 1°C throughout the 9-yr history.

All these models had cells of constant length ΔX_i. A more efficient procedure would be to increase ΔX_i progressively with depth below the bottom contact. We did not do so because linear interpolation was more convenient, and the one-dimensional calculations were not costly in computer time. In more refined calculations, however, variable cell lengths would be advisable.

Source functions for the latent heat of crystallization.—Analytical methods incorporating the latent heat of crystallization have been extensively discussed in the papers by Jaeger. For cooling of magma bodies, these methods involve simplifying assumptions of one sort or another. It is well established, however, that the effect of latent heat not only slows cooling but also increases temperatures at contacts over the values calculated for cooling models without heat sources. Jaeger (1964) has shown

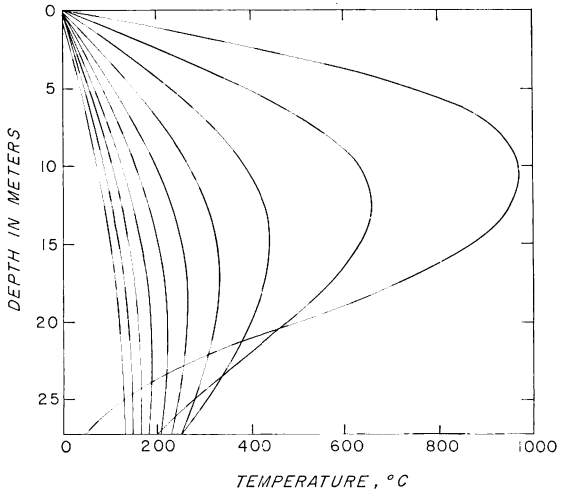

Fig. 3. Cell balance calculation of temperature profiles for an extrusive sheet with no sources and thermal diffusivity D = 0.0118 (compare Ingersoll, Zobell, and Ingersoll, 1954, fig. 7.5, p. 99). Sheet thickness is 20 m, ΔX_i = 50 cm, *UINF* = 0 at 60 m. Profiles are at 1/4, 1, 2, 3, 4, 5, 6, 7, 8, and 9 yrs.

that calculated contact temperatures are sensitive to the way the latent heat is included in the analysis. He also showed that the best of known analytical solutions is obtained by applying Neumann's solution for the progress of a solidification boundary (Carslaw and Jaeger, 1959, §11.2) with an effective heat capacity based on averaging the latent heat over the temperature range of crystallization.

The cell balance method has the advantage of greater flexibility in assigning relations between the amount of latent heat, the amount of crystallization, and temperature. As a result, it should potentially give more realistic temperature distributions within the uncertainties of approximations in incremental calculations discussed above. Therefore, we are interested in testing how the numerical results differ from those of the analytical method, when similar assumptions are made about the release of latent heat; also we will test how nonlinear distributions, based on knowledge of crystallization intervals, may further modify temperature profiles and contact temperatures. In this and the next section, we define functions for the latent heats of crystallization and vaporization of rain and then discuss comparisons with the previous analytical methods.

In our derivation of source functions for the latent heat of crystallization of Alae lake, we were guided by petrographic studies of crystallization sequences versus temperature. In detail, the latent heat distribution depends on the phases crystallizing, the net crystallization rates, and densities of the solidified lava. Textural studies have shown, however, that nucleation and growth rates for lava lakes are sufficiently similar that there is not much modal variation for the known ranges of cooling rates. Therefore, we can make the quasi-equilibrium assumption that the

volume fraction of crystallized phases depends only on temperature. This assumption does not necessarily imply chemical equilibrium among the phases, and, in fact, there is a small residual fraction of melt that remains as interstitial glass in the solidified lava.

In the derivation of the heat source function, we define the following quantities (no confusion exists for the crystallization and vaporization source functions, so we use no special subscripts):[1]

L	latent heat per unit mass for change from entirely liquid to crystalline states,
ΣQ^*	latent heat per unit volume for change from entirely liquid to entirely crystalline states ($= LP_i$),
Φ_i	volume fraction of crystals,
$\Delta\Phi_i$	change in volume fraction of crystals during a time step,
$\Sigma\Phi_i$	total change in volume fraction of crystals between specified initial and final states,
ΔQ_i^*	amount of latent heat deposited during a time step,
LUV_i^*	the ratio $\Delta Q_i^*/P_iC_i$,
$\Delta UXLIZ$	temperature interval of crystallization,
U_1	initial temperature of crystallization interval for magma of given crystal content, and
U_2	lower temperature of crystallization interval for given crystal content.

In the general case, we might wish to specify several crystallization intervals, if there are marked nonlinearities in the amount of crystallization for a given temperature change or if the heats of crystallization of the various mineral phases are markedly different. Accordingly, U_1 and U_2 would be suitably identified for the upper and lower bounds of each interval. First, however, we will illustrate the method by assuming a linear distribution over a single interval for Alae lava; later, we will divide the range into three intervals. At temperature U_1, the lava already contains some fraction of crystals, and at temperature U_2, there is some residual fraction of melt quenched as glass. For the case of Alae lava, $U_1 = 1140°C$ and $U_2 = 980°C$; the initial crystallinity at U_1 is $\Phi = 0.13$, and the final crystallinity at U_2 is $\Phi = 0.93$. Accordingly at any temperature U in the crystallization range, the volume fraction of crystals is

$$\Phi = 0.13 + \frac{1140 - U}{\Delta UXLIZ}\,\Sigma\Phi;\ 980 \leqslant U \leqslant 1140°C, \tag{6}$$

where

$$\Delta UXLIZ = 160°C, \text{ and } \Sigma\Phi = 0.80.$$

[1] In this section temperatures with numerical subscripts refer to crystallization ranges, not to cell temperatures. During computation these temperatures are introduced numerically.

The change in crystallinity for a given temperature decrease during a time step is defined by

$$\Delta\Phi_i = \frac{-\Delta U}{\Delta UXLIZ}\ \Sigma\Phi, \tag{7}$$

where the minus sign is included because the ΔU values are negative, and the $\Delta\Phi_i$ values are positive. The total available latent heat for the range $\Sigma\Phi$ is $\Sigma\Phi\Sigma Q^* = 0.80LP_i$ for the above distribution. Therefore, the heat released in a cell during the time step is given by

$$\Delta Q_i^* = \frac{-\Delta U_i}{\Delta UXLIZ}\ \Sigma\Phi\Sigma Q^* V_i = -0.80\ LP_i V_i\ \frac{\Delta U_i}{\Delta UXLIZ}\ . \tag{8}$$

This expression is introduced in eq (4) by virtue of the identity $LUV_i^* = \Delta Q_i^*/P_iC_i$. Combining and rearranging terms gives the adjusted expression for the temperature change:

$$\Delta U_i = \frac{P_iC_i\Delta UXLIZ}{P_iC_i\Delta UXLIZ + \Sigma\Phi\Sigma Q^*}\left(\frac{LUV_{i+1} - LUV_i}{V_i}\right)\ ;\ U_2 \leqslant U_i \leqslant U_1. \tag{9}$$

The term on the right outside the parentheses is called Heat of Crystallization Coefficient and is given the symbol *HXC*. This coefficient for a single linear crystallization interval for Alae becomes (the density term disappears when the latent heat is expressed per unit mass)

$$HXC = \frac{C_i\Delta UXLIZ}{C_i\Delta UXLIZ + \Sigma\Phi L}\ ;\ 980 \leqslant U_i \leqslant 1140°C, \tag{10}$$

with $\Sigma\Phi = 0.80$ as defined above.

As a numerical example, if L = 100 cal g^{-1} for complete transformation from the liquid to crystalline states, then the fraction 0.80 or 80 cal g^{-1} is available for the actual crystallization interval. For $\Delta UXLIZ$ = 160°C and C_i = 0.3 cal $g^{-1}°C^{-1}$, we obtain *HXC* = 0.375. It must be specified in the program, of course, that this coefficient is applied only in those cells with temperatures between 980° and 1140°C.

Petrographic studies of drill core samples of Alae lava indicate that the relation of crystallinity to temperature is significantly nonlinear. A second approximation to the actual distribution is defined by dividing the total interval above into three parts. Higher order approximations can be derived by further subdivision and by expressing the total latent heat L in terms of the heats of crystallization of the individual minerals. Here we simply assume that L is proportioned according to the variations of crystallinity without regard to the phases crystallizing.

For the sake of illustration, suppose the three intervals are defined in terms of temperature and crystallinity as follows:

Interval 1 $U_1 = 1140, U_2 = 1070; \Phi_1 = 0.13, \Phi_2 = 0.33$

Interval 2 $U_1 = 1070, U_2 = 1040, \Phi_1 = 0.33, \Phi_2 = 0.73$

Interval 3 $U_1 = 1040, U_2 = 980; \Phi_1 = 0.73, \Phi_2 = 0.93$

The three crystallization coefficients are then obtained from eq (10) by introducing the appropriate values of $\Delta UXLIZ$ and $\Sigma\Phi$ for each interval. For the first interval, $\Delta UXLIZ = 70$, and $\Sigma\Phi = 0.2$, and so on.

Accordingly, we have $HXC\ 1 = 0.512$, $HXC\ 2 = 0.184$, and $HXC\ 3 = 0.474$. These coefficients are substituted in eq (4) for those cells having temperatures within the respective intervals defined above.

Various crystallization coefficients and sets of coefficients were used in trial runs for Alae lake. Discussion of the values finally adopted is given in part II, although we found, in general, that refinement beyond three intervals was not warranted.

Source functions for the vaporization of rain.—Rainfall in the vicinity of Kilauea Volcano is generally abundant, averaging roughly 250 cm per yr. The effect on cooling of lava, particularly near the upper surface, clearly is significant if water can percolate very deep along joint cracks or through interconnecting vesicles and cavities. If there were no penetration of the rock, rainfall would pose no major problem to the model, because then it would simply act as an agent of surface heat transfer that maintains the surface at an approx constant temperature, just as does the convective circulation of air in the absence of rain.[2]

The effect of penetration of the lava by rain can be viewed in two different ways. If there were an independent way to specify the depth of penetration of an isothermal surface (for example, the 100°C isotherm) as a function of time, then this condition could be imposed directly as an upper boundary condition that changes in position with time. Cooling would be enhanced because temperature gradients immediately below this isothermal boundary would be steepened relative to values computed for a stationary isothermal boundary.

In the absence of rigorous criteria to specify such a moving boundary condition, we chose to assume that rain uniformly penetrates the lava until it reaches the boiling point and then vaporizes and totally escapes to the atmosphere without recondensation at shallower depths in the lava. In this sense, rainfall can be considered as an instantaneous negative heat source within each cell that reaches 100°C, moving progressively downward from the upper surface. This assumption provides an indirect way to specify a moving boundary condition that is automatically determined by the heat balance equations.

In detail, the physical processes implied by our assumption are quite complex. The circulation of water and steam within the various joint sets and other connected openings in lava suggests that depths of penetration will be irregular over the lake surface and that there should be

[2] We neglect consideration of radiation effects on surface temperatures and the transient effects of variations in the efficiency of heat transfer across the lava-air interface. In our calculations, we assume surface temperatures based on temperature measurements across the interface. These temperatures are somewhat higher than ambient air temperature and, in effect, represent a correction for radiation effects and for surface resistance to air cooling. If knowledge of temperatures or heat flux distributions across the surface warranted, such data could be directly substituted as surface boundary conditions. For discussion of surface temperatures, see Peck (in press).

substantial opportunity for partial recondensation. We find, however, that for Alae lake (pt. II) the principal features of the cooling history are reproduced rather well by assuming total vaporization of the recorded rainfall without accounting for either the depth variation of penetration or recondensation.

In thicker lava lakes, however, there is evidence for partial recondensation early in the cooling history and evidence for nearly complete recondensation after a certain stage of cooling. In that event, the effect may be accounted for by introducing a positive heat source for condensation of steam as well as a negative heat source at the depth of boiling. Such a system resembles on a small scale the vapor-dominated geothermal systems of White, Muffler, and Truesdell (1971).

Rainfall records in the vicinity of Alae lake were used as input from which the amount of vaporization heat was summed for a given choice of time step. This quantity is defined by

$$\Delta Q_i^* = A\Sigma R, \tag{11}$$

where A is the cell area at the lava surface (unity in the one-dimensional model), and ΣR symbolizes the integrated heat of vaporization per unit area during a time step ΔT. The quantity ΔQ_i^* is entered directly as a source term in eq (4) in the form $LUV_i^* = \Delta Q_i^*/P_iC_i$. The ratio LUV_i^*/V_i is the temperature drop of the cell equivalent to the magnitude of the heat of vaporization during a time step. The temperature drop, of course, depends on both the size of the cell and the size of the time step. Values of the integrated heat per unit area ΣR are based on a heat of vaporization of 620 cal/cm^3. This represents the sum of the heat of vaporization at the boiling point and the heat absorbed in bringing the water to that temperature from ambient air temperatures.

Trial calculations for different values of ΔX_i and ΔT show that the potential temperature drop may be excessively large, if ΔT is too large. A test for the maximum allowable ΔT can be introduced by specifying a maximum allowable temperature drop. Ordinarily this would be a temperature drop such that the value of ΔU_i obtained from eq (4) will not give a temperature for that cell less than the cell immediately above, although temperature reversals could be physically possible depending on the rate of penetration and degree of superheating of the water.

For simplicity, we specified that the heat of vaporization was removed from that cell (moving progressively downward from the surface) that first reached 100°C based on linear interpolation between mean temperatures of adjacent cells. This gave adequate results, and any spurious temperature gradients could be eliminated by repeated trials with smaller time increments.

A more rigorous method is to remove the heat of vaporization from the cell that first reaches 100°C based on linear interpolation, but in which the temperature drop does not cause the mean temperature to fall below 100°C. If this condition is not met, the heat of vaporization

is removed from the cell immediately below. Results using this assumption did not differ significantly from those based on a simple linear test for the position of the 100°C isotherm for the Alae analysis. In other cases, however, it may be important to include the additional tests.

TRIAL RUNS FOR ALAE

The remainder of the paper describes some of the effects obtained by varying the different input parameters. In most of these runs, we used a one-dimensional model analogous to figure 3 with cell lengths of 30.48 cm (1 ft) and with time step of $\Delta T = 3.237 \times 10^4$ sec (0.385 days). The lake depth was taken to be 14.6 m (48 ft), though we tested effects of thickness variations of about a meter. We maintained a lower boundary condition at two sheet thicknesses below the bottom contact and assigned $UINF = 20°C$ at a depth of 45 m below the surface.

Strategy of analysis.—We can illustrate only a few of the many trial runs that were made, and therefore we outline here some of the effects they were designed to test. Examples of sets of computed profiles are given in figure 4. Detailed fitting of the calculated profiles to measured temperatures are illustrated in part II. The profiles in figure 4 are given at those times for which temperature measurements were made in drill holes.

Figure 4A illustrates results obtained for a constant diffusivity of 0.006 $cm^2\ sec^{-1}$ (approx the best mean value for this lava lake) without incorporation of heat sources and sinks. This result is directly analogous to figure 3; that is, it resembles early attempts to describe cooling of lava flows such as the example illustrated by Ingersoll, Zobel, and Ingersoll (1954). Figure 4B gives results allowing for a total of 80 cal g^{-1} latent heat distributed linearily over the crystallization interval, whereas figure 4C distributes the same total latent heat in three intervals for the same constant diffusivity. In figure 4D, we have added the effect of vaporization of rain with diffusivity still constant, and figure 4E illustrates the same result with diffusivity proportional to temperature. These profiles (fig. 4A through E) at three different times after formation of the lake (75.5, 379.7, and 1010.4 days) are compared in figure 4F.

These profiles illustrate that the latent heat of crystallization (regardless of the distribution) and vaporization of rain are the dominant controls on total cooling times and shapes of profiles. Changes in the distribution of latent heat affect profile shapes only very slightly at temperatures above the solidus. Variable diffusivity also changes the profile shapes slightly but significantly.

The effect of vaporization of rain as a moving boundary condition is shown dramatically in figures 4D and 4E by the breaks in slope near 100°C and their rates of penetration with time. Comparison of figure 4B or C with 4D and E shows that in the absence of rainfall cooling to 100°C takes about five times longer (about 20 versus 4 yrs). Cooling without either sources or sinks falls between these limits.

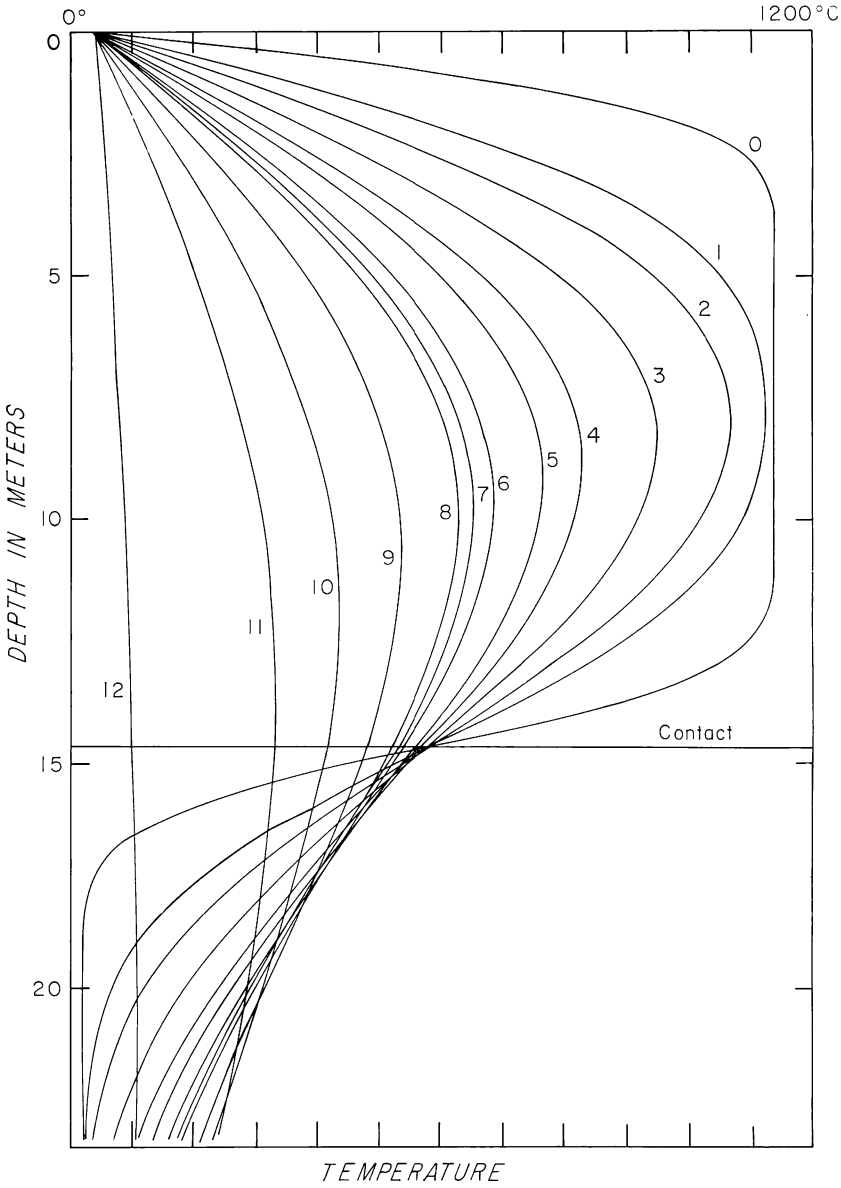

Fig. 4. Examples of trial runs for Alae lava lake. Thickness was tentatively assumed to be 14.6 m. The emplacement temperature is 1140°C, the upper contact temperature is 40°C, and initial temperatures below the lake are 20°C. Profiles are shown for different assumptions: (A) no heat sources, constant thermal diffusivity D = 0.006 cm^2sec^{-1}; (B) D = 0.006, latent heat of 80 cal g^{-1} distributed linearly between 1140° and 980°C; (C) D = 0.006, latent heat of 80 cal g^{-1} distributed in three parts; (D) same as (C) with addition of heat of vaporization of rain; (E) same as (D) with thermal

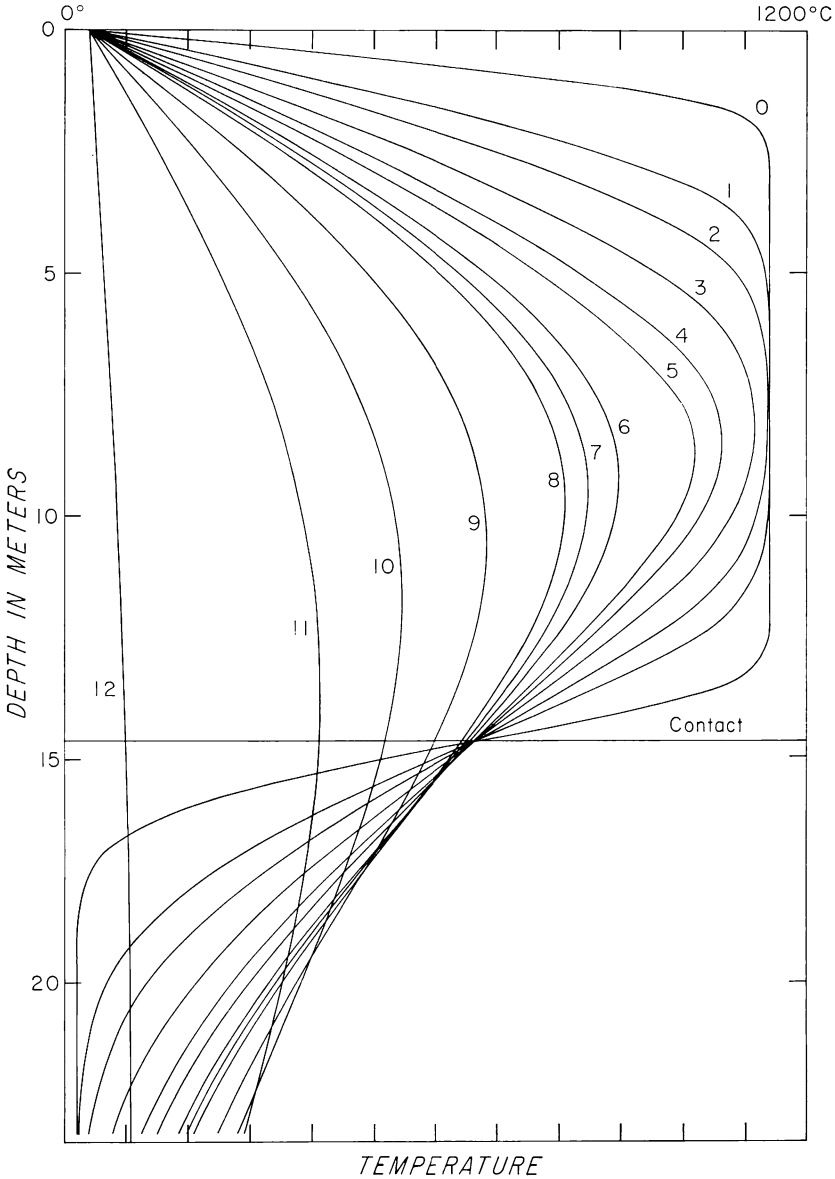

B.

conductivity proportional to temperature; (F) profiles 1, 5, and 10 from A (shortest dashes), B and C (medium dashes), D (long dashes), and E (solid lines) are compared. Profiles were computed at the following times (in days) after formation of the lake: 15.0, 75.5, 129.6, 216.4, 316.1, 379.7, 475.6, 519.8, 559.1, 729.3, 1010.4, 1471.0, and 7129.6. The effect of rain was computed on the basis of the recorded rainfall plotted in figure 2 of part II.

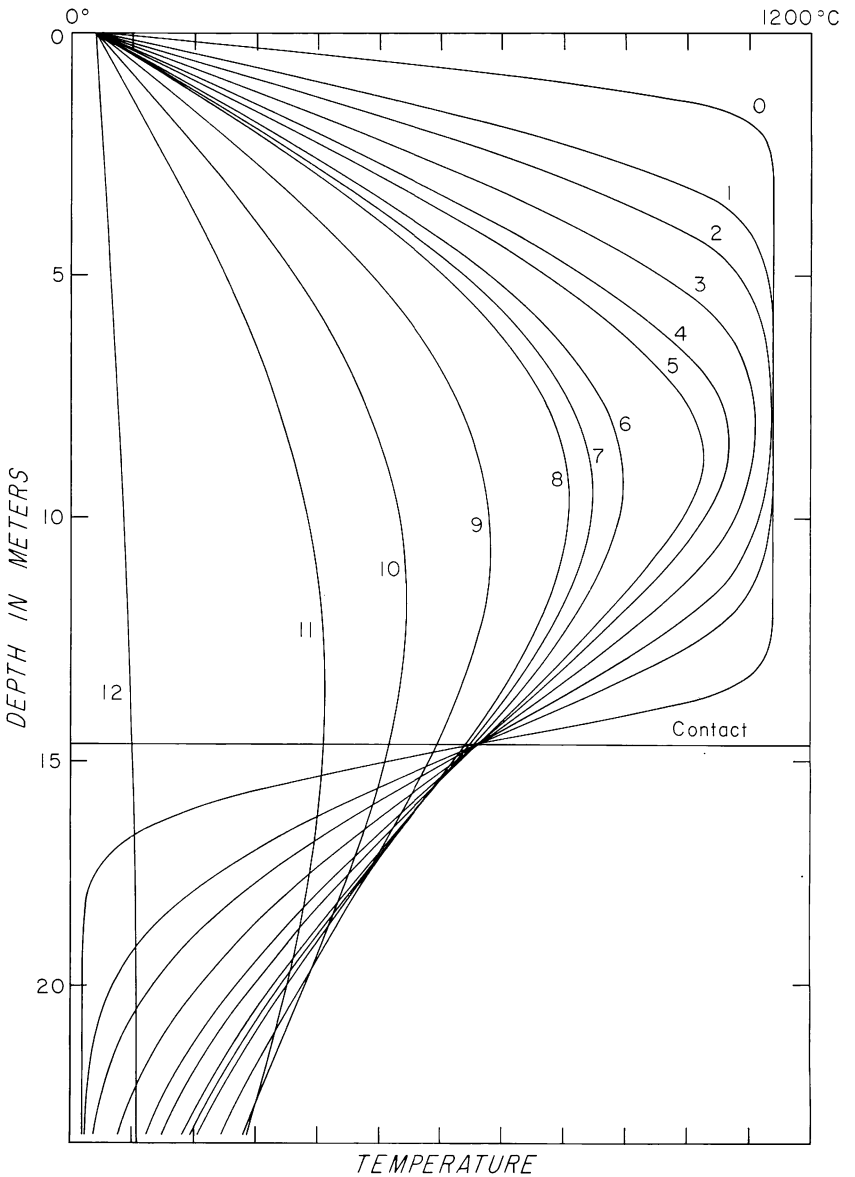
0°
1200°C
0
5
10
15
20
DEPTH IN METERS
TEMPERATURE
Contact
0
1
2
3
4
5
6
7
8
9
10
11
12

C.

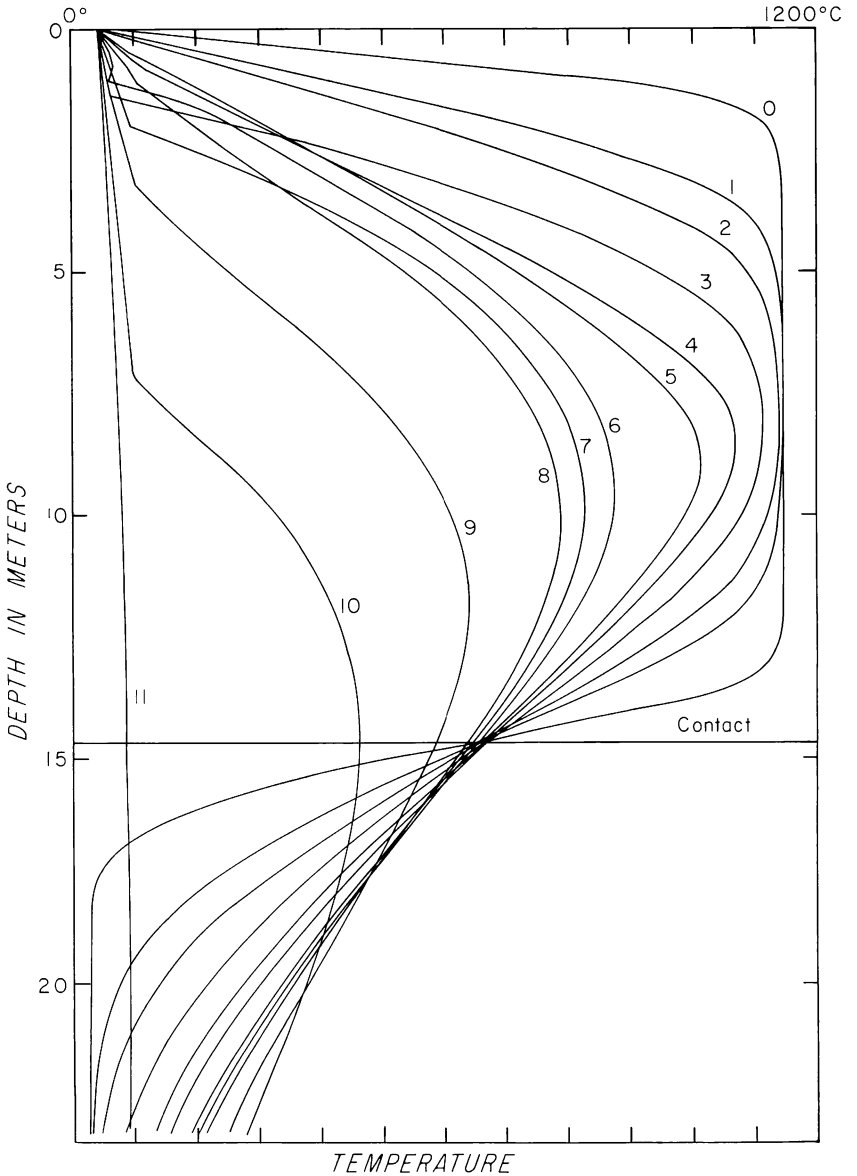
0°
1200°C
0
5
10
15
20
DEPTH IN METERS
TEMPERATURE
0
1
2
3
4
5
6
7
8
9
10
11
Contact

D.

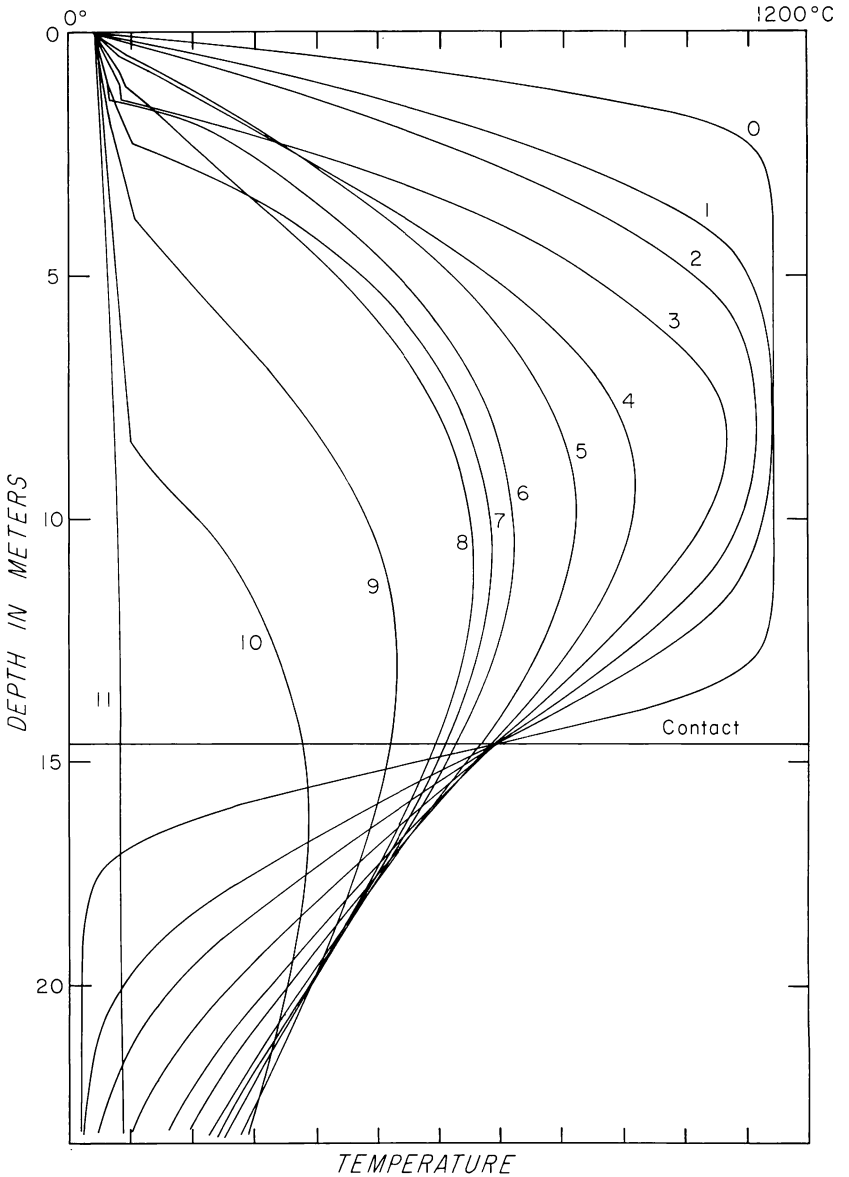
0°
1200°C
0
5
10
15
20
DEPTH IN METERS
TEMPERATURE
Contact
0
1
2
3
4
5
6
7
8
9
10
11

E.

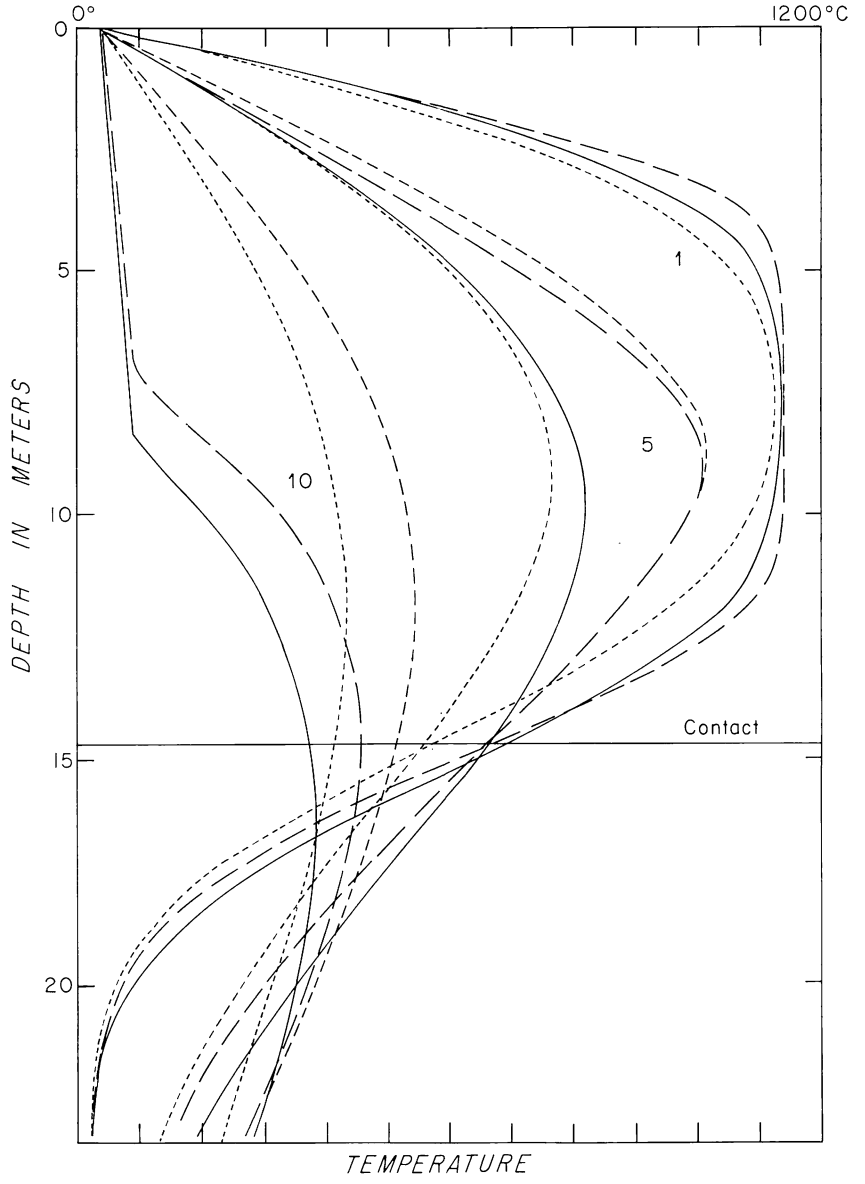

F.

Some of the profiles at intermediate times in figure 4D and E cross over earlier profiles. This feature is caused by the irregularities in rainfall. Initially, rainfall was very light followed by a very heavy period, then by a light period, and again by a relatively heavy period (upper part of fig. 2 of part II). The quenching effect of the first period of heavy rainfall partly recovered during the following light period, which caused transient reversals of cooling in the upper part of the lake.

By manipulating computer runs to emphasize different cooling regimes, we were able to test which parameters had to be varied to give agreement with temperature data. For example, the earliest profiles were dominated by dependence of conductivities on steep gradients of temperature and porosity near the upper surface as well as on the choice of latent heat. This is because initially there was a very small cooling effect from the vaporization of rain because of the very light rainfall. On the other hand, profiles following complete crystallization were dominated mainly by the choice of mean diffusivity and the cooling effect of vaporization of rain. Profiles between the earliest and the subsolidus profiles were dominated by the choice of latent heat for a given mean diffusivity determined from the subsolidus history and lake thickness. The choice of latent heat additionally was influenced by the computed temperatures at the lower contact, which at that stage of cooling were independent of the effects of vaporization of rain and so on. The details of these manipulations, the temperature data, and the physical factors they reflect are discussed at length in part II.

Comparison with the analysis by Jaeger; contact temperatures.—Jaeger (written commun. to Peck, 1967) was the first to attempt fitting the data for Alae lake by a combination of analytic and numerical methods. In essence his approach consisted of three parts: (A) computation of the progress of a solidification front using Neumann's solution (Carslaw and Jaeger, 1959, chap. 11); (B) computation of subsolidus cooling using a one-dimensional finite difference method with 10 cells in the lake; (C) trial and error adjustments of constant thermal properties.

The assumption of the Neumann solution is that there is a moving planar interface between a solid and liquid phase of different thermal properties and with release of the latent heat of crystallization at the melting temperature. Jaeger (1957) showed that this solution could be employed for magmatic crystallization by incorporating the latent heat in an effective heat capacity for the crystallization interval. The solution holds only so long as crystallization can be approximated by the one-dimensional semi-infinite assumption; that is, the magma temperature at central positions in the body is constant, and the solidification front moves at a rate proportional to the square root of time. Therefore, the assumption begins to fail for finite bodies when the maximum temperature (*UMAX*) begins to fall below the initial temperature. Also, the crystallization interval represents a finite depth interval, and that interval increases with time, as is evident by inspection of figure 4 for the

temperature range 980° to 1140°C. Therefore, the Neumann solution is not entirely realistic, and this factor appears to have a small but significant effect on calculated contact temperatures.

Figure 5 shows the maximum and contact temperatures versus time as computed by Jaeger and by us given a constant diffusivity of 0.006 cm^2sec^{-1} and a latent heat of 80 cal g^{-1}. Jaeger divided the lake into ten cells 1.37 m long because the mean thickness of the lake is approx 13.7 m. Our results in figure 5 with 0.3 m cell lengths are for the same

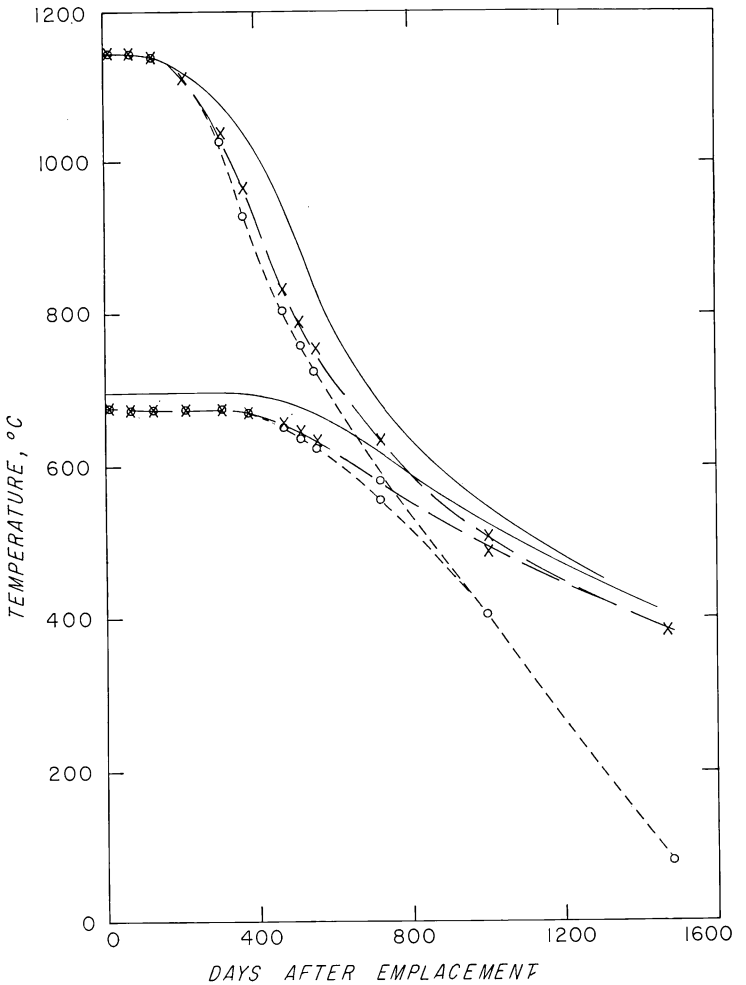

Fig. 5. Comparison of maximum temperatures (upper set) and contact temperatures (lower set) between our results and those of Jaeger (written commun., 1967) for a lake 13.7 m (45 ft) thick with a diffusicity of 0.006 cm^2/sec and a latent heat of 80 cal/g. Solid line, Jaeger no-rain model. Long dashed line and crosses, our no-rain model. Short dashed line and circles, our model incorporating the measured rainfall for Alae lava lake.

lake thickness, though most of our other runs were made using a thickness appropriate to the vicinity of the drill holes where temperature measurements were made (part II). Jaeger did not explicitly account for rainfall effects, so we have shown results with and without the heat of vaporization removed.

The principal distinctions are that our initial contact temperatures are 20°C lower than his, and both the maximum and contact temperatures begin to fall off sooner than his. He terminated his calculation at about 4 yrs, so we cannot show comparisons at longer times, but eventually there should be a crossover in order to compensate for the initial differences, if the overall heat balances are correctly incorporated. Possibly the effect of the large grid size used in his calculations could account for the differences after solidification in a manner analogous to our earlier discussion of comparisons of our coarse-grid computations with the exact solution of Ingersoll, Zobel, and Ingersoll (1954). Jaeger's results after solidification more nearly resemble ours for a 14.6 m lake, suggesting the possibility of interpolation errors. Initial maximum and contact temperatures for the 14.6 m lake, however, are the same, and the 20°C difference in initial contact temperature presumably reflects the difference between the Neumann assumptions and our fine-grid numerical solutions. The vaporization of rain does not influence the early maximum and contact temperatures but does, of course, eventually cause them to fall off much faster than in the "no rain" models.

Jaeger's analysis was normalized relative to a uniform initial boundary temperature of 40°C, and we used the same assumption in figure 5. The lower boundary condition, however, is closer to 20°C, and we used that condition in other runs, so any comparisons require adjustments for the different total temperature ranges. Relative to an initial reference condition with zero degrees at the surface and contacts, Jaeger's results are equivalent to using an initial lava temperature of 1100° instead of 1140°C. On this basis, his initial contact temperature is 0.595 of the emplacement temperature given a latent heat of 80 cal g^{-1}. On the same basis, our initial contact temperature is 0.577 of the emplacement temperature.

Jaeger (1964) discusses the effects of different analytical assumptions and values of latent heat on calculated maximum and contact temperatures. Both his and our results show that initial contact temperatures increase roughly 1°C for each increase in latent heat of 1 cal g^{-1}. Thus, our results for $L = 80$ cal g^{-1} are approx equivalent to those using the Neumann solution with a latent heat of about 60 cal g^{-1}. Assuming that the fine-grid numerical solutions are more realistic than the Neumann solutions, the implicit initial contact temperatures should be about 3 percent lower than those advocated in the papers by Jaeger; that is, 0.60 instead of 0.62 of the initial temperature when $L = 100$ cal g^{-1}, 0.58 instead of 0.60 when $L = 80$ cal g^{-1}, and so on.

The differences indicated by figure 5 and the above discussion are *not* very significant relative to general temperature distributions and

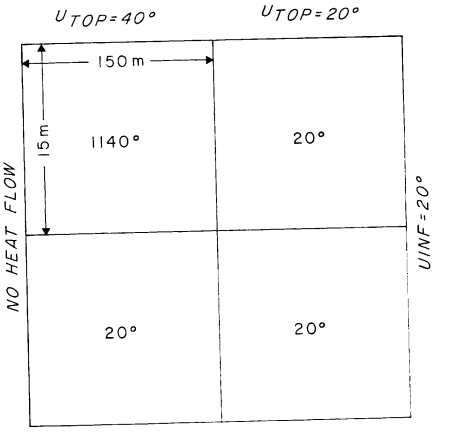

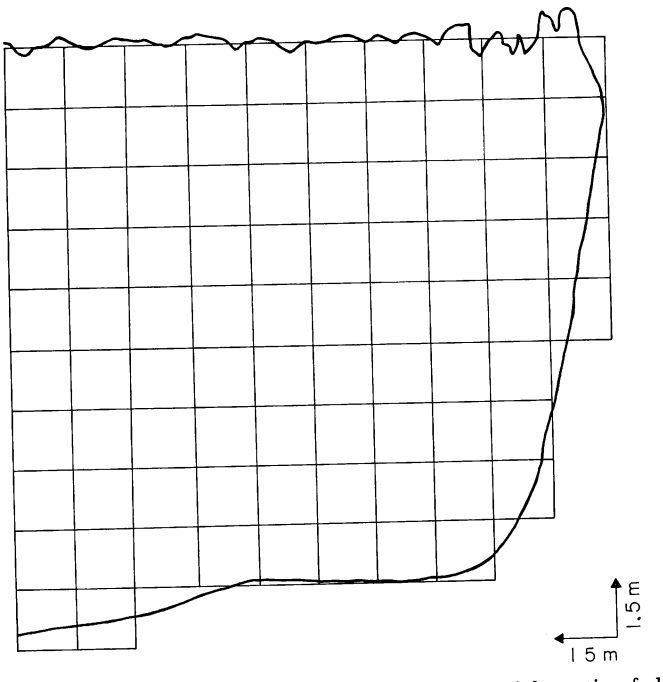

Fig. 6. Grid system for two-dimensional calculations. A. Schematic of dimensions, original temperature distribution, and boundary conditions. B. Generalized radial section of Alae lava lake (10 × vertical exaggeration) showing the assignment of cells.

cooling times, but they might be significant in special cases where detailed contact effects are being considered. Although we have no absolutely rigorous basis for stating that our numerical result is correct, it does more closely represent latent heat distributions during crystallization. It also gives predicted contact temperatures in agreement with the measurements in Alae lake, but this is not a strong confirmation because of uncertainties in the exact location of the contact and properties of the rocks immediately below.

Coarse-grid solutions in two dimensions; cooling from the margins.—In order to test the validity of the one-dimensional profiles during the recorded history of Alae, we made two-dimensional analyses with cells 1.5 m vertically and 15 m horizontally. Figure 6 illustrates the cell distribution. We took the mean half-width across the central part of the lake and assumed a no-flow boundary condition at the center. Computation is initiated at the top center cell, performs all the cell balances along the top row, and then moves progressively downward in the same manner as the one-dimensional balances of table 1.

The display of results takes various forms. Initially, we were interested in plotting temperature arrays and profiles at the center for the same time intervals as in the cases illustrated earlier. These comparisons show that the effects of lateral cooling have not modified the one-dimensional results near the center during the 4-yr history. The results and cross sections showing the progress of selected isotherms are illustrated and discussed in part II (fig. 9 and p. 431 and 432).

CONCLUSIONS

We conclude here and in part II that computer analysis of lava lake cooling histories by the method of explicit cell balances gives excellent simulation of the observational data and can be refined to almost any desired computational accuracy. The method permits new discrimination among possible ranges of thermal properties of basaltic lava found in the literature, as discussed in part II. There are, however, remaining uncertainties about thermal diffusivity, latent heat, and vaporization-condensation reactions of ground water that will require additional modeling of other lava lakes. Clearly, the method also provides a versatile approach for testing many other models of heat conduction or models of chemical diffusion.

ACKNOWLEDGMENTS

We thank Professor Norman Davids of the Pennsylvania State University for discussion of computer methods. The manuscript was reviewed by T. L. Wright, A. H. Lachenbruch, and E-an Zen of the U.S. Geological Survey, and by M. P. Ryan of the Pennsylvania State University. Helpful comments also were given by D. R. Wones and C. R. Faust of the U.S. Geological Survey, and by H. C. Hardee and D. W. Larson of Sandia Laboratories.

References

Berger, R. L., and Davids, Norman, 1965, General computer method of analysis of conduction and diffusion in biological systems with distributive sources: Rev. Sci. Instruments, v. 36, p. 88-93.

Boydell, H. C., 1932, Temperature of formation of an epithermal ore deposit: London, Inst. Mining Met. Trans., v. 41, p. 458-522.

Carslaw, H. S., and Jaeger, J. C., 1959, Conduction of Heat in Solids: Oxford, Clarendon Press, 510 p.

Davids, Norman, and Berger, R. L., 1964, A computer analysis method for thermal diffusion in biochemical systems: Communications of Am. Computer Machine Soc., v. 7, p. 547-551.

Desai, C. S., and Abel, J. F., 1972, Introduction to the Finite Element Method: New York, Van Nostrand Reinholt Co., 477 p.

Gruntfest, I. J., 1963, Thermal feedback in liquid flow; plane shear at constant stress: Rheology Soc. Trans., v. 7, p. 195-207.

Hess, G. B., 1973, Heat and mass transport during crystallization of the Stillwater Igneous Complex: Geol. Soc. America Mem. 132, p. 503-520.

Hess, H. H., 1960, Stillwater Igneous Complex, Montana: Geol. Soc. America Mem. 80, 230 p.

Hsu, S. T., 1963, Engineering Heat Transfer: Princeton, N.J., Van Nostrand Co., 613 p.

Ingersoll, L. R., Zobel, O. J., and Ingersoll, A. C., 1954, Heat Conduction: Madison, Univ. Wisconsin Press, 325 p.

Irvine, T. N., 1970, Heat transfer solidification of layered intrusions; I. Sheets and sills: Canadian Jour. Earth Sci., v. 7, p. 1031-1061.

Jaeger, J. C., 1957, The temperature in the neighborhood of a cooling intrusive sheet: Am. Jour. Sci., v. 255, p. 306-318.

———— 1964, Thermal effects of intrusions: Rev. Geophysics, v. 2, p. 443-466.

———— 1968, Cooling and solidification of igneous rocks, *in* Hess, H. H., and Poldervaart, Arie, ed., Basalts. v. 2: New York, Interscience Pub., p. 503-536.

Larsen, E. S., 1945, Time required for the crystallization of the great batholith of southern and lower California: Am. Jour. Sci., v. 243A, p. 399-416.

Lovering, T. S., 1955, Temperatures in and near intrusions: Econ. Geology, v. 50, p. 249-281.

McAdams, W. H., 1954, Heat Transmission: New York, McGraw-Hill, 532 p.

McBirney, A. D., 1959, Factors governing emplacement of volcanic necks: Am. Jour. Sci., v. 257, p. 431-448.

Peaceman, D. W., and Rachford, H. H., 1955, The numerical solution of parabolic and elliptic differential equations: Soc. Indus. Appl. Math. Jour., v. 3, p. 28-41.

Peck, D. L., in press, Cooling and vesiculation of Alae lava lake, Hawaii: U.S. Geol. Survey Prof. Paper 935B, in press.

Peck, D. L., Moore, J. G., and Kojima, George, 1964, Temperatures in the crust and melt of Alae lava lake, Hawaii, after the August 1963 eruption of Kilauea Volcano —A preliminary report: U.S. Geol. Survey Prof. Paper 501-D, p. D1-D7.

Price, P. H., and Slack, M. R., 1954, The effect of latent heat on numerical solutions of the heat flow equation: British Jour. Appl. Research, v. 5, p. 285-287.

Provost, A., and Bottinga, Yan, 1972, Rates of solidification of Apollo 11 basalt and Hawaiian tholeiite: Earth Planetary Sci. Letters, v. 15, p. 325-337.

Reilly, W. I., 1958, Temperature distribution about a cooling volcanic intrusion: New Zealand Jour. Geology and Geophysics, v. 1, p. 364-374.

Richter, D. H., and Moore, J. G., 1966, Petrology of the Kilauea Iki lava lake, Hawaii: U.S. Geol. Survey Prof. Paper 537-B, p. B1-B26.

Rikitake, T., 1959, Studies of the thermal state of the earth; 2. Heat flow associated with magma intrusion: Tokyo Univ., Earthquake Research Inst. Bull., v. 37, p. 233-243.

Shaw, H. R., 1965, Comments on viscosity, crystal settling, and convection in granitic magmas: Am. Jour. Sci., v. 263, p. 120-152.

———— 1969, Rheology of basalt in the melting range: Jour. Petrology, v. 10, p. 510-535.

———— 1974, Diffusion of H_2O in granitic liquids: Part I, Experimental data; Part II, Mass transfer in magma chambers: Carnegie Inst. Washington Pub. 634, p. 139-170.

Siekierka, W. J., ms, 1971, Thermal feedback in liquid flow using finite-element methods: M.S. thesis, Eng. Mech., June 1971, Pennsylvania State Univ.

Strang, Gilbert, and Fix, G. J., 1973, An analysis of the Finite Element Method: Englewood Cliffs, N.J., Prentice-Hall, Inc., 306 p.

White, D. E., Muffler, L. J. P., and Truesdell, A. H., 1971, Vapor-dominated hydrothermal systems compared with hot-water systems: Econ. Geology, v. 66, p. 75-97

Wright, T. L., Peck, D. L., and Shaw, H. R., 1976, Kilauea lava lakes: Natural laboratories for study of cooling, crystallization, and differentiation of basaltic magma: Am. Geophys. Union Geophys. Mon. 19, p. 375-390.